Sensors & Actuators: B. Chemical 367 (2022) 132182

Contents lists available at ScienceDirect

Sensors and Actuators: B. Chemical

journal homepage: www.elsevier.com/locate/snb

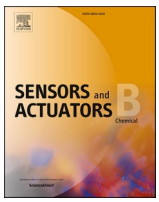

Monitoring rapid metabolic changes in health and type-1 diabetes with breath acetone sensors

Andreas T. Güntner [a,b,*], Ines C. Weber [b], Stephanie Schon [b], Sotiris E. Pratsinis [b], Philipp A. Gerber [a,**]

[a] Department of Endocrinology, Diabetology, and Clinical Nutrition, University Hospital Zurich (USZ) and University of Zurich (UZH), CH-8091 Zurich, Switzerland
[b] Particle Technology Laboratory, Department of Mechanical and Process Engineering, ETH Zurich, CH-8092 Zurich, Switzerland

ARTICLE INFO

Keywords:
Nanotechnology
Electronics
Wearables
Metabolism
Medicine

ABSTRACT

Routine detection of health parameters is desirable to recognize the early onset of metabolic diseases (e.g., diabetes mellitus) and to personalize their treatment. Promising are non-invasive, affordable and portable technologies, such as breath sensors. Yet, the selective monitoring of breath markers (e.g., acetone for lipolysis) with sensors to track metabolic changes that can reveal disease-related abnormalities remains challenging. Here, subtle breath acetone changes during fasting, exercise and glucose ingestion are tracked in two model situations: Patients suffering from type-1 diabetes mellitus (T1DM) and healthy subjects (total: 19 volunteers) were monitored using chemoresistive sensors based on Si/WO_3 nanoparticles. Specifically, each subject cycled after overnight fasting to stimulate fatty acid oxidation followed by an oral glucose tolerance test (OGTT), as monitored by capillary blood glucose and β-hydroxybutyrate (BOHB) concentrations. The sensor recognized accurately the *individual* breath acetone patterns before and after OGTT (both $R^2 = 0.9$) at negligible interference, for instance, from glucose ingestion-associated volatiles (e.g., ethanol) or isoprene, as confirmed by high-resolution mass spectrometry. Furthermore, distinct differences in the breath acetone patterns of T1DM over healthy subjects were revealed including higher (*t*-test, $p = 0.006$) breath acetone ratio 2 h after starting the OGTT. Worth noting is that after glucose intake, breath isoprene steadily increased for T1DM subjects while it remained rather constant for healthy ones, an intriguing observation that requires more research to clarify its biochemical origin and medical relevance.

1. Introduction

The longitudinal assessment of changes in metabolic parameters is a promising tool for the detection of metabolic diseases, monitoring of body homeostasis, or self-assessment of the effectiveness of lifestyle changes on metabolism [1]. The variety of such metabolic diseases is large, from rare (and difficult to detect) inborn disorders of biochemical processes (such as glycogen storage diseases or phenylketonuria) to much more prevalently acquired diseases like diabetes mellitus, dyslipidemia, or fatty liver disease. In order to develop tools that allow such assessment, individual health parameters need to be monitored longitudinally [2] to recognize abnormal patterns [1] and indicate the status of interventions (e.g., diets and exercise). To date, however, monitoring of the metabolism is largely impractical and inefficient [3].

Breath analysis is attractive being non-invasive, thus highly tolerable, rapid (if done online [4]), and exhaled breath is always accessible. Most importantly, breath compounds can reflect immediate metabolic changes. [5] In recent years, emphasis has been placed on monitoring the fat metabolism through breath acetone [6], a by-product of fatty acid oxidation (Fig. 1a, left) [7]. More specifically, end-tidal breath acetone levels increased typically from few hundreds of parts-per-billion (ppb) to tens of parts-per-million (ppm) during fasting [8] and correlated [9] to the duration of ketogenic dieting [10], reflecting enhanced fatty acid oxidation, as confirmed by simultaneous blood ketone measurement (i.e., BOHB). Furthermore, subtle acetone increases were observed during physical activity [11] (moderated by cardiorespiratory fitness [12]) and post-exercise rest [13]. Finally, breath tests after overnight fasting revealed no direct relationship between blood glucose and breath

* Corresponding author at: Department of Endocrinology, Diabetology, and Clinical Nutrition, University Hospital Zurich (USZ) and University of Zurich (UZH), CH-8091 Zurich, Switzerland.
** Corresponding author.
E-mail addresses: Andregue@ethz.ch (A.T. Güntner), Philipp.gerber@usz.ch (P.A. Gerber).

https://doi.org/10.1016/j.snb.2022.132182
Received 15 February 2022; Received in revised form 25 April 2022; Accepted 6 June 2022
Available online 8 June 2022

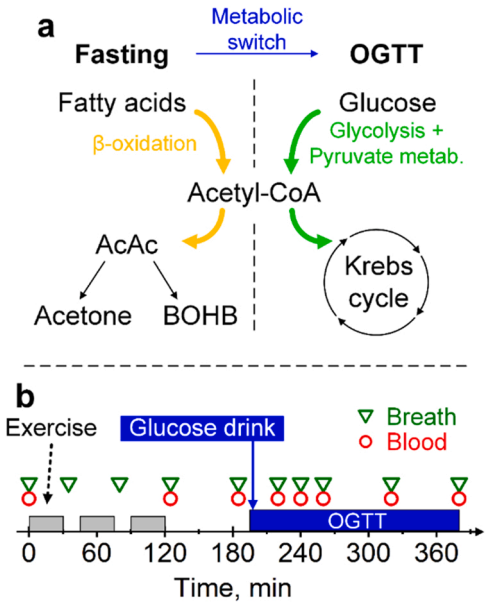

Fig. 1. (a) Metabolic pathway of fatty acid oxidation (left) and glucose (right) breakdown. During fasting, fatty acids are converted to acetyl coenzyme A (acetyl-CoA) which diverts to the ketone bodies acetoacetate (AcAc), β-hydroxybutyrate and volatile acetone. During glucose breakdown, the resulting acetyl-CoA is metabolized in the Krebs cycle and no acetone is formed. (b) The test protocol starts with three sessions of 30 min exercise each (gray shaded) after overnight fasting and subsequent post-exercise rest to stimulate fatty acid oxidation. Afterwards, an OGTT (blue shaded) is performed to induce rapidly the change to glucose metabolism. Breath (triangles) and blood (circles) were measured throughout the protocol.

acetone concentrations together with no significant differences between healthy and type-2 diabetes mellitus patients (T2DM) [14]. However, when tested additionally 1 h later during an OGTT (i.e., 75 g glucose intake), the breath acetone ratio in T2DM differed from the healthy subjects [14], revealing disease-related metabolic abnormalities when switching fuel preference from fatty acids to glucose.

Most promising to track such breath acetone dynamics online and routinely are chemical sensors [15] that can be extremely compact [16], operated at low-power [17] and integrated into hand-held and communicative devices [18]. Several sensor types showed promising performance for acetone detection including adsorption columns [19], enzyme-based assays [20], conductive polymers [21], colorimetric [22], chemoresistive semiconductors (e.g., porous SnO_2 spheres [23], Al/ZnO nanoparticles [24], Co_3O_4/PdO-loaded In_2O_3 [25] and Cr [26] or WO_3 nanoparticles doped with Si [27] or Nb [28] nanoparticles alone or pre-screened by Pt/Al_2O_3 [29] catalytic packed bed filters [30]) and arrays [31] that enabled even the detection of additional breath tracers (e.g., isoprene, ammonia [32], ethanol [33]). Only few sensors/arrays had been applied already to track the breath acetone dynamics during calorie-restricted [19,31], fat-rich (i.e., ketogenic) [34] and carbohydrate-rich diets [22], as well as during fasting [22]. Even finer acetone changes during constant- [13] and ramped-load [35] cycling were monitored online [36] with Si/WO_3 sensors. Therein, this sensor showed high acetone selectivity over various compounds (e.g. ethanol, isopropanol, CO or H_2) in laboratory gas mixtures [37] as well as a bias and precision of 271 and 442 ppb, respectively, when quantifying the breath acetone concentration in real breath [35]. Nevertheless, more challenging breath acetone dynamics in healthy and T1DM subjects during a rapid metabolic switch (Fig. 1a) have not been tracked with such compact sensors yet.

Here, we evaluate a flame-made [38] chemoresistive sensor's ability to track rapid and fine breath acetone changes when switching fuel preference from fatty acid oxidation to glycolysis (Fig. 1a) in 13 healthy and 6 T1DM subjects. T1DM is characterized by an absolute deficiency in insulin, one of the most important regulator hormones of carbohydrate metabolism. Thereby, T1DM served as a model disease for disturbed carbohydrate metabolism. To this end, the overnight-fasted subjects performed three times 30 min exercise at moderate intensity [13] to stimulate fatty acid oxidation followed by an OGTT. Fatty acid and glucose metabolism were monitored by parallel blood BOHB and glucose measurements, respectively. Smallest end-tidal breath acetone changes were measured online with (1) a portable gas sensor based on Si/WO_3 nanoparticles [27] and (2) a proton transfer reaction time-of-flight mass spectrometer (PTR-TOF-MS) [39] to identify the sensor's robustness to endogenous volatiles (e.g., ethanol, isoprene) formed, for instance, from glucose ingestion and released by muscle activation. Finally, differences in the metabolic marker profiles between the healthy and T1DM subgroups were assessed statistically.

2. Experimental section

2.1. Participants

Twenty T1DM and healthy adults aged 20–36 years were recruited for this study. Participants had to be free of respiratory and cardiovascular diseases. This study was approved by the Kantonale Ethikkommission Zürich (#2015-0675). Each subject gave written consent to the protocol with the opportunity to abort the test or withdraw consent anytime.

2.2. Study protocol

The experimental protocol is illustrated schematically in Fig. 1b. Prior to the test, the participants were asked to fast overnight for 12 h, abstain from alcoholic drinks and physical activity for 24 h, and avoid tooth brushing for 2 h to minimize exogenous influences. T1DM patients were instructed to administer basal insulin using their usual dosage.

The test started at 8 a.m. with measurements of the subject's weight and height to calculate the body mass index (BMI) and weight-specific insulin dose. Next, three times 30 min cycling at moderate intensity was performed on an ergometer (E5, Kettler) followed by 1 h of post-exercise rest [13]. Exercise intensity was regulated automatically by the ergometer through workload adjustment to keep a constant heart rate (HR, measured via a pulse belt H7 Polar) at 63 % [40] of the maximum one (HR_{max}). The latter was approximated for men using $HR_{max} = 223 - 0.9 \times$ [age] and for women using $HR_{max} = 226 -$ [age] [41] (age in years, HR in beats per minute). In a second stage, an OGTT was performed by administering 75 g anhydrous glucose dissolved in 375 mL of water within 5 min, as recommended by the World Health Organization (WHO) for diabetes testing [42]. This was followed by 3 h of rest.

Breath samples (triangles, Fig. 1b) were collected before the exercise, after each 30 min cycle as well as after 1 h of post-exercise rest. After each cycle, the participants rested for 5 min before taking breath and blood samples. After the glucose drink, breath was sampled every 20 min in the first hour and hourly thereafter. Throughout the whole study, the subjects continued fasting being allowed only to drink water apart from the glucose intake. Capillary blood samples (circles) were obtained immediately after each breath measurement. Between the exercise cycles, no blood was sampled to minimize the subject's discomfort.

2.3. Breath analysis

End-tidal breath was extracted in a standardized and reproducible fashion with a tailor-made [43] sampler. Therein, subjects exhaled for 30 s into the sampler while maintaining an airway pressure of 980 Pa and expiration flow rate of 50 mL s^{-1}, as recommended by the American Thoracic/European Respiratory Societies for nitric oxide [44]. During

exhalation, the CO_2 concentration was monitored (Capnostat 5, Respironics) to ensure that the subjects reached the end-tidal breath portion ($CO_2 > 3$ % [45]). Breath samples were extracted continuously from the sampler via a heated Teflon transfer line to the acetone sensor and a high-resolution PTR-TOF-MS 1000 (Ionicon Analytik, Austria). The transfer line was heated to 65 °C to avoid analyte adsorption and water condensation.

The acetone sensor is based on Si/WO_3 nanoparticles with its fabrication described elsewhere [36]. Such a sensor was mounted on a Macor holder, installed inside a Teflon chamber and fed from the breath sampler with a constant flow of 130 mL min^{-1} by a vane pump (SP 135 FZ, Schwarzer Precision) connected to the chamber outlet [13]. The sensor substrate's Pt heater was connected to a DC power source (R&S, HMC8043, Germany) to heat the sensor to an operating temperature of 350 °C (~ 6.5 W), as optimized before for selective acetone sensing [36]. This temperature was monitored continuously using the back-heater as resistance temperature detector. Sensor resistance was recorded using a multimeter (Keithley 2700). The sensor response to extracted breath samples was defined as [27].

$$S_{breath} = \frac{R_{air}}{R_{breath}} - 1$$

where R_{air} and R_{breath} are the sensor resistances in surrounding room air and when exposed to breath samples, respectively. Sensor responses were averaged from three consecutive breath samples.

The PTR-TOF-MS was connected in parallel to the acetone sensor and fed with a constant flow of ca. 50 mL min^{-1} from the same transfer line to avoid interference by inter-sample variation. It was operated at a drift voltage, temperature and pressure of 600 V, 60 °C and 2.3 mbar, respectively. The reduced electric field in the drift tube (E/N) was 130 Td using H_3O^+ as precursor ions and the resolution was 1584 m/fwhm (at $m/z = 59.05$), as measured and in agreement with the instrument's technical specification [46]. After data acquisition, a mass calibration was done at $m/z = 21.02$ [47] and 37.03 [47]. Acetone concentrations were measured at a mass-charge ratio (m/z) of 59.05 [48] by comparison of the signal intensity to three-point calibrations obtained from calibrated gas cylinders (10 ppm acetone in synthetic air, Pan Gas 6.0) at 90 % relative humidity with a gas mixing set-up described elsewhere [49]. In addition, relative changes in ethanol and isoprene were evaluated at $m/z = 47.05$ [48] and 69.07 [50], respectively. Note that isopropanol was not analysed, as its signal overlapped with that of acetic acid.

2.4. Blood analysis

Capillary blood was obtained by finger pricking using lancet pens (Abbott Diabetes Care, UK). Glucose and BOHB were determined with a FreeStyle Neo Precision (Abbott Diabetes Care, UK).

2.5. Data analysis

Statistical analysis was performed using OriginPro (2018G, OriginLab Corporation, Massachusetts, USA), except for the receiver operating characteristic (ROC) analysis, that was done with SPSS Statistics 28 (IBM, Armonk, USA). Subgroup characteristics were expressed through means and standard deviations (SD). Agreement analysis between sensor and PTR-TOF-MS was conducted based on Pearson's correlation coefficients (r), coefficient of determinations (R^2) and Bland-Altman analysis [51]. Descriptive analysis of the breath acetone, isoprene, ethanol ratios, blood BOHB and glucose concentrations included means and standard error of the mean. Therein, normalized breath acetone, isoprene and ethanol were obtained by normalization to the baseline concentrations to account primarily for effects of the protocol (Fig. 1b). Independent two-sided t-test were performed to compare the healthy and T1DM subgroups. The level of significance level was set at $p \leq 0.05$.

3. Results & discussion

3.1. Subgroup characteristics

In total, nineteen subjects finished the experimental protocol of the study with demographic and anthropometric characteristics summarized in Table 1 and individually listed in Table S1. One of the 20 recruited participants had to be excluded due to non-compliance with the physical activity prohibition within 24 h prior to the test. Thirteen subjects were healthy in the sense that no prior metabolic disease had been diagnosed before the trial. Six participants had been diagnosed with T1DM 12.5 ± 7.6 years before the test and were treated with insulin (mean 0.59 ± 0.27 insulin units kg^{-1} day^{-1}) confirming their normal [52] insulin sensitivity. In general, both subgroups featured comparable (t-test, $p > 0.5$) young age of 25.3 ± 3.2 (healthy) and 26.8 ± 5.3 years (T1DM) and BMI of 23.2 ± 2.5 and 22.6 ± 2.8 kg m^{-2}, respectively. While the T1DM subgroup contained a larger share of female participants (67 vs. 31 %), previous studies observed no gender-related differences for breath acetone [53].

3.2. Comparison between sensor and PTR-TOF-MS

First, we assessed the sensor's accuracy by comparing it to high-resolution PTR-TOF-MS. Fig. 2a shows the normalized breath acetone before (triangles) and during the OGTT (circles) of the 190 breath samples, as measured by both instruments. Note that the breath acetone is normalized (i.e., sensor response ratio with respect to the initial value at $t = 0$) to assess only the effects of the interventions for an easier comparison between the subjects, in agreement with previous studies [13,14]. This normalized breath acetone can be converted into acetone concentration after prior sensor calibration with gas standards [35].

Before the OGTT, the sensor correlates linearly (Pearson's correlation coefficient $r = 0.95$) with PTR-TOF-MS featuring high coefficient of determination ($R^2 = 0.9$), sufficiently small limits of agreement (Fig. 2b, dashed lines) and negligible systematic bias (solid line, i.e., mean difference), as revealed also by Bland-Altman analysis [51]. Comparable results ($r = 0.97$) had been obtained in a previous test with the same instruments on 20 healthy subjects (i.e., 280 breath samples) following a similar fasting and exercise protocol [13]. Only at high normalized breath acetone (i.e., > 3), the sensor tends to underpredict it (Fig. 2a, dashed vs. solid line). The response characteristics of such chemo-resistive sensing films follow diffusion-reaction theory [54]. At elevated analyte concentration, the analyte diffusion inside these films and the adsorption on the constituent nanoparticle surfaces become non-linear [55]. This results in non-linear response characteristics, as was observed experimentally for SnO_2 with CO [55] and the same Si/WO_3 when tracking breath acetone during ketogenic diets [34].

Most importantly, the high correlation ($r = 0.95$) and coefficient of determination ($R^2 = 0.9$) between sensor and PTR-TOF-MS is preserved during the OGTT (circles, Fig. 2). Thus, the sensor seems quite robust to endogenous ethanol concentrations, in agreement with gas standard measurements [36], that increase rapidly after glucose intake (Fig. S1a) probably due to fermentation of carbohydrates by gut bacteria and yeast in the gastrointestinal tract [56]. The sensor is also hardly affected by isoprene, that gradually increased during the post-exercise rest and OGTT (Fig. S1b). This is shown even better when juxtaposing the individual normalized breath acetone, isoprene and ethanol profiles

Table 1
Demographic and anthropometric data of the subjects. Average values for the healthy and T1DM group are presented as mean ± SD.

Group	Female	Age [years]	Number [-]	BMI [kg m^{-2}]
Healthy	31 %	25.3 ± 3.2	13	23.2 ± 2.5
T1DM	67 %	26.8 ± 5.3	6	22.6 ± 2.8

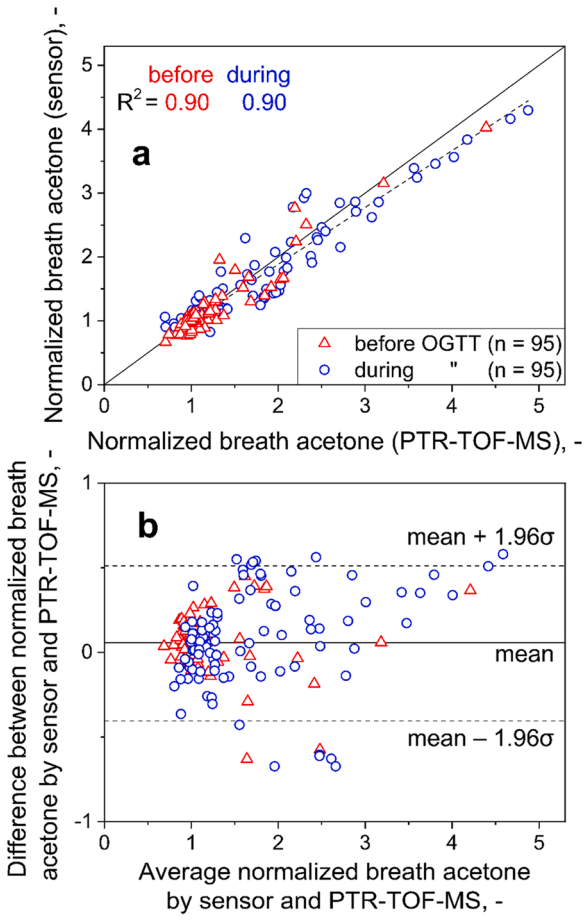

Fig. 2. (a) Normalized breath acetone (normalized to the initial concentration) measured by the sensor and PTR-TOF-MS before (triangles, n = 95) and during the OGTT (circles, n = 95) on 19 subjects. The ideal line (solid line) and the linear fit (dashed line) for all samples are indicated. (b) Bland-Altman analysis between sensor and PTR-TOF-MS measurements. The solid line represents the mean difference and the dashed lines the limits of agreement (1.96 times the SD).

exemplarily for subjects #1, 2 & 9 (healthy) as well as #15, 17 & 18 (T1DM) in Fig. S2 where the sensor and PTR-ToF-MS measurements mostly overlap. Hence, the Si/WO_3 sensor is well suited (overall R^2 = 0.9, Fig. 2a) to track the breath acetone dynamics during fasting, exercising and OGTT, as will be explored next. Note that higher ethanol concentrations (sometimes released from disinfectants in clinical environments) or isoprene spikes that occur few minutes after starting the exercise [11] can interfere this Si/WO_3 sensor [35]. However, this can be mitigated by placing catalytic packed beds [30] of Pt/Al_2O_3 [29] ahead of such sensors and was even exploited for selective isoprene tracking when combining it with a sorption filter of activated alumina [57].

It is worth comparing also the sensor performance between healthy (squares, Fig. S3a) and T1DM (inverted triangles). More specifically, sensor and PTR-TOF-MS correlate similarly well for healthy (r = 0.96) and T1DM (0.94). Furthermore, Bland-Altman analysis (Fig. S3b) did not reveal significant differences with respect to systematic bias or limits of agreement. Therefore, the sensor's accuracy to detect breath acetone is also not affected by T1DM in the present setting, despite probably different breath compositions. In fact, a previous study with a larger cohort (n = 113) of children reported, for instance, higher concentrations of ethanol, isopropanol, dimethylsulfid, isoprene and pentanal in the T1DM subjects [58].

3.3. *Healthy subjects: Individual metabolic marker profiles during exercise and OGTT*

Fig. 3a shows the normalized breath acetone of the representative, healthy subjects #1 (circles), #2 (squares) and #9 (triangles), as determined by the portable sensor (filled symbols) and PTR-TOF-MS (open symbols). During exercise and post-exercise rest (0–185 min), all subjects feature distinctly different breath acetone profiles. For instance, breath acetone hardly changes for subject #9, while it increases significantly already during exercise in case of #1 and reaches more than fourfold levels at the end of the post-exercise rest. Such large inter-subject variation has been observed before [13] and reflects differences in the activation of fatty acid oxidation, for instance, due to differences in current glycogen stores, or cardiorespiratory fitness [12].

This is confirmed also by simultaneous blood BOHB measurements (Fig. 3b), another by-product of fatty acid oxidation (Fig. 1a, left) and an established clinical marker [59], that shows similar trends to breath acetone (Fig. 3a), in agreement with literature [60]. Therefore, fuel preference is clearly on fatty acid oxidation at the end of the exercise and post-exercise rest, as was targeted by this protocol and confirmed also by the low glucose levels (i.e., < 5.6 mM, Fig. 3c). In fact, subject #1 is

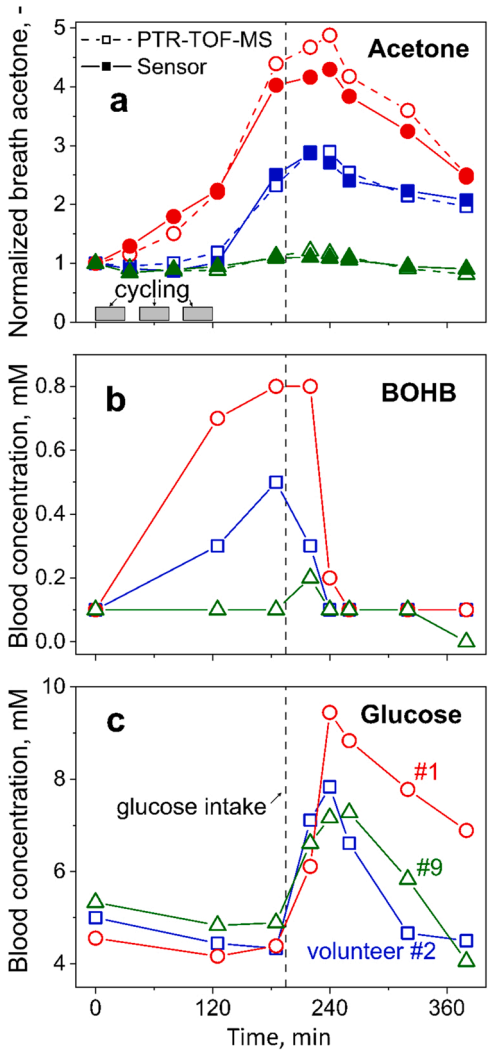

Fig. 3. (a) Normalized breath acetone measured by the sensor (filled symbols) and PTR-TOF-MS (open symbols), as well as capillary blood (b) BOHB and (c) glucose levels for representative healthy subject #1 (circles), 2 (squares) and 9 (triangles). The grey boxes (in a) indicate the exercise cycles and the vertical dashed lines the glucose intake (i.e., start of OGTT at t = 185 min).

entering even nutritional ketosis (i.e., BOHB: 0.5–3 mM [61], Fig. 3b) at the end of the post-exercise rest. Most importantly, the sensor (Fig. 3a, filled symbols) accurately tracked these individual fat metabolism dynamics online through non-invasive breath acetone measurements, in excellent agreement with PTR-TOF-MS (open symbols) and in line with Fig. 2a.

When starting the OGTT (t > 185 min, vertical dashed line, Fig. 3c), the blood glucose concentrations rapidly increase in all subjects and peak at 7.3–9.4 mM within 40–60 min after glucose ingestion. Thereafter, they decrease until the end of the test, as expected for healthy subjects. Simultaneously, blood BOHB levels rapidly drop to 0.1 mM (Fig. 3b) indicating a rapid metabolic switch from fatty acid oxidation to glycolysis (Fig. 1a). Most importantly, this is also reflected by breath acetone (Fig. 3a) that decreases in concentration upon reaching peak glucose levels (Fig. 3c), consistently for all subjects though less pronounced for subject #9. The sensor's ability to resolve such rapid and fine metabolic switches has immediate practical impact: For instance, non-compliance to ketogenic diet protocols (e.g., wrong selection of nutrients) can be easily detected.

Finally, it is worth discussing that BOHB levels (Fig. 3b) drop faster upon glucose intake than the respective acetone concentrations (Fig. 3a). Similar observations were made after insulin administration during the treatment of diabetic ketoacidosis. [62] This might be associated to acetone's hydro- and lipophilic properties leading to its accumulation in body fluids and slow elimination primarily through exhaled breath [62] with a partition coefficient in lung alveoli (blood:air) of 126:1 [63]. In contrast, BOHB can be metabolized further in extrahepatic mitochondria [64]. As a result, breath acetone is less sensitive to sudden metabolic changes, in agreement with our observation in Fig. 3a, b.

3.4. T1DM-related differences

Finally, we compared the healthy and T1DM subgroups to investigate whether breath acetone reflects differences in metabolic constitution, as established with blood glucose [65]. In fact, after overnight fasting (at t = 0 min), the glucose concentrations are higher in the T1DM (mean: 8.5 mM, Table S1) compared to the healthy subgroup (4.9 mM). Values in all T1DM subjects exceeded 7 mM, probably reflecting insufficient suppression of endogenous glucose production by the basal insulin administered. Also, the corresponding breath acetone concentrations (1814 vs. 987 ppb, Table S1) and blood BOHB (0.22 vs. 0.1 mM) tend to be higher, indicating an incomplete insulin-mediated suppression of ketogenesis. While individual breath acetone levels were significantly higher (max. 3′364 ppb) in some T1DM subjects than in the healthy volunteers (max. 1′484 ppb), both subgroups were statistically not distinguishable ($p = 0.148$).

Therefore, we investigated the dynamics for breath acetone (Fig. 4a), blood BOHB (b) and glucose (c) during the exercise and OGTT stimuli when metabolic differences between the subgroups should be more pronounced. More specifically, the increase in normalized breath acetone during exercise and post-exercise rest is lower for the T1DM (i.e., 1.3, circles, at 185 min) compared to the healthy (1.9, triangles) subgroup, as indicated by the sensor. This agrees with the blood BOHB concentrations, where a smaller increase was observed also for the T1DM (0.22–0.35 mM) compared to the healthy (0.1–0.38 mM) subgroup. While insulin production is increasingly suppressed in healthy subjects during exercise, in T1DM subjects, the acting basal insulin is fixed, which should be responsible for the decreased flexibility of their metabolism.

The most striking difference was observed during the OGTT. Specifically, the breath acetone continues to increase in the T1DM subgroup, while it decreases (after t = 240 min) in the healthy subgroup, where the endogenous insulin response takes place, as observed also in Fig. 3a. This is confirmed somehow by BOHB levels that decrease in the T1DM subgroup during the OGTT, though with some delay (i.e., after

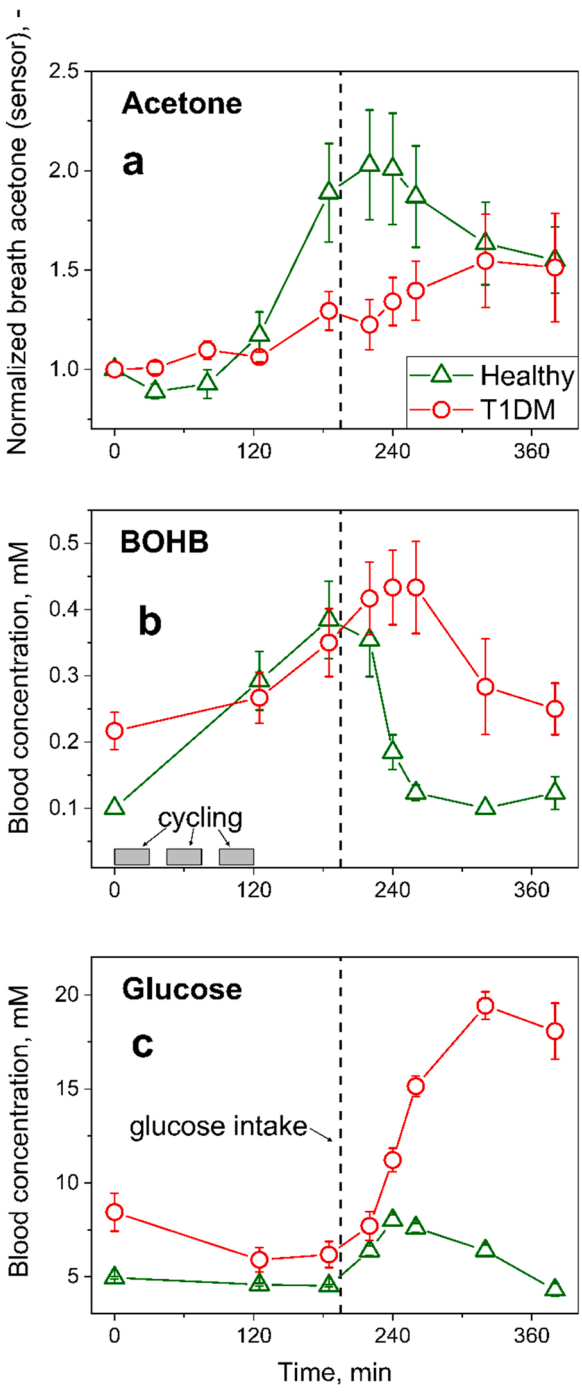

Fig. 4. (a) Normalized breath acetone (normalized to the initial acetone concentration of each subject), blood (b) BOHB and (c) glucose concentrations in the healthy (triangles, n = 13 subjects) and T1DM (circles, n = 6 subjects) groups. Symbols and error bars indicate the mean and standard error of the mean values. Note that the normalized breath acetone was measured by the sensor. The grey boxes (in b) indicate the exercise cycles and the vertical dashed lines the glucose intake (i.e., start of OGTT at t = 185 min).

t = 255 min) and less distinct compared to the healthy subgroup. As expected, all subjects show distinct increases in blood glucose (Fig. 4c) upon glucose intake. Significantly higher levels are observed for the T1DM, that peaked (16.1 – 21.3 mM) 2 h after the glucose intake (dashed line, Fig. 4c), compared to the healthy subjects, where blood glucose does not exceed 8.7 mM.

This can be exploited to distinguish healthy subjects (Fig. 5a: left boxed and whiskers) from T1DM patients (right boxes and whiskers)

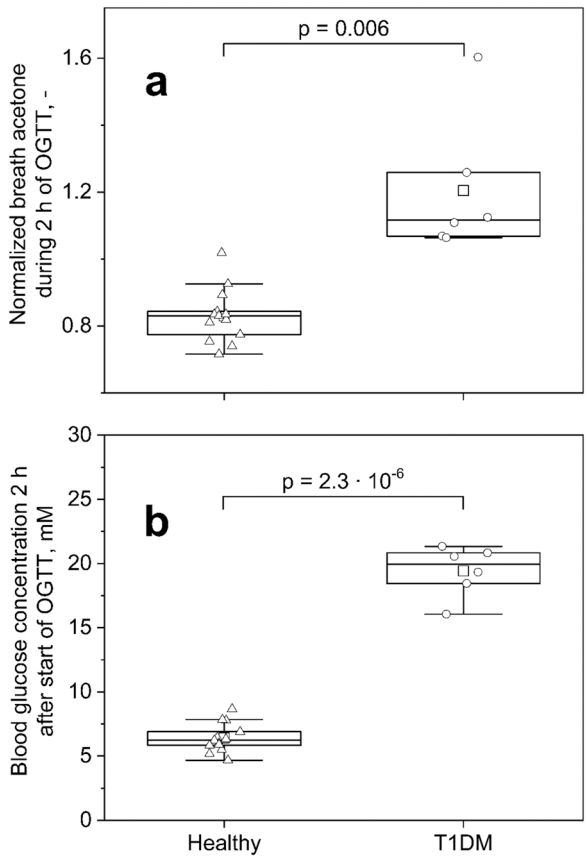

Fig. 5. Box-whisker plots for (a) normalized breath acetone (normalized to the start of the OGTT, i.e., t = 185 min) and (b) glucose concentration after 2 h of the OGTT, following the American Diabetes Association guidelines for the diagnosis of diabetes through blood glucose [65]. Note that the normalized breath acetone was measured by PTR-ToF-MS. Individual data points are shown for the healthy (triangles) and T1DM (circles) subjects, with symbols outside the whiskers representing outliers.

with the sensor. Therefore, the normalized breath acetone is formed by normalization to the start of the OGTT (i.e., t = 185 min; not t = 0 min as done for Figs. 2–4) and evaluated 2 h after glucose intake (i.e., t = 305 min). The normalized breath acetone distinguished ($p = 0.006$) the T1DM from the healthy subgroup, similar to the standard blood glucose test ($p = 2.6 \bullet 10^{-6}$, Fig. 5b). When choosing an appropriate discrimination threshold for a ROC analysis, high medical specificity and sensitivity (e.g. both 100 % at a normalized breath acetone of 1.04) can be obtained for the discrimination of health and disease. Note that also absolute breath acetone concentrations (measured by PTR-TOF-MS) tend to be higher ($p = 0.053$, Table S2) in the T1DM subgroup 2 h after glucose intake. These results highlight the present breath acetone sensor's ability to recognize disease-related abnormalities by tracking metabolic markers. As a result, it can be promising for screening and management of metabolic diseases, though this must be confirmed with larger cohorts in clinical trials in different settings of disease.

Note that differences between healthy and T1DM adults were observed also in the breath ethanol and isoprene profiles (Fig. S1), as measured by PTR-TOF-MS. For instance, the mean ethanol levels peaked at higher value (2.8 vs. 2 at t = 240 min) during the OGTT for the T1DM compared to healthy subjects. Furthermore, the mean breath isoprene level increased steadily during post-exercise rest and OGTT for the T1DM subjects (e.g., 2.1 vs. 1.1, Table S2) while it remained rather constant for healthy ones 2 h after glucose intake. However, further research is required with larger cohorts and clarify also the biochemical origin and medical relevance of these differences.

4. Conclusion

The online tracking of fine breath acetone dynamics during fasting, exercise, rest and glucose intake was demonstrated with a portable sensor in healthy and T1DM subjects. Thereby, the sensor recognized individual breath acetone patterns with high accuracy and precision, as confirmed by high-resolution mass spectrometry. This suggests high acetone selectivity over endogenous volatiles (e.g., ethanol from glucose ingestion or exercise-related isoprene). That way, disease-related differences between healthy and T1DM adults (as a model of metabolic diseases) were captured, providing new insights for the interpretation and clinical utility of breath acetone in the context of metabolic malfunctions. Also the sensor's ability to resolve rapid and fine metabolic switches can help to detect compliance to ketogenic diet protocols. This low-cost sensor can be readily integrated into battery-driven and communicative devices [18] for personalized feed-back on metabolism in healthy and diseased populations.

CRediT authorship contribution statement

Andreas T. Güntner: Conceptualization, Methodology, Formal analysis, Investigation, Writing – original draft, Writing – review & editing, Visualization, Supervision, Funding acquisition. **Ines C. Weber:** Formal analysis, Investigation, Writing – review & editing, Visualization. **Stephanie Schon:** Methodology, Formal analysis, Investigation. **Sotiris E. Pratsinis:** Methodology, Investigation, Writing – review & editing, Visualization, Supervision, Funding acquisition. **Philipp A. Gerber:** Conceptualization, Methodology, Investigation, Writing – review & editing, Visualization, Supervision.

Declaration of Competing Interest

The authors declare the following financial interests/personal relationships which may be considered as potential competing interests: Andreas T. Guentner reports a relationship with Alivion AG that includes: board membership and equity or stocks. Andreas T. Guentner and Sotiris E. Pratsinis has patent issued to ETH Zürich.

Acknowledgments

We thank S. Jonathan Theodore for assistance with the measurements, Sebastian Abegg for help with the data evaluation & figure design (both ETH Zürich) and Noriane Sievi & Malcolm Kohler for supporting the clinical implementation of this investigation. This study was supported financially by ETH Zürich (Research Grant ETH-05 19-2), the Swiss National Science Foundation (159763, 170729 & 175754), the University Hospital Zürich Innovationspool (INOV00117), the Uniscientia Foundation (173-2020) and the Stiftung Accentus – Verena Guggisberg-Lüthi Fonds.

Appendix A. Supporting information

Supplementary data associated with this article can be found in the online version at doi:10.1016/j.snb.2022.132182.

References

[1] N.D. Price, A.T. Magis, J.C. Earls, G. Glusman, R. Levy, C. Lausted, D.T. McDonald, U. Kusebauch, C.L. Moss, Y. Zhou, S. Qin, R.L. Moritz, K. Brogaard, G.S. Omenn, J. C. Lovejoy, L. Hood, Nat. Biotechnol. 35 (2017) 747.

[2] S.M. Schussler-Fiorenza Rose, K. Contrepois, K.J. Moneghetti, W. Zhou, T. Mishra, S. Mataraso, O. Dagan-Rosenfeld, A.B. Ganz, J. Dunn, D. Hornburg, S. Rego, D. Perelman, S. Ahadi, M.R. Sailani, Y. Zhou, S.R. Leopold, J. Chen, M. Ashland, J. W. Christle, M. Avina, P. Limcaoco, C. Ruiz, M. Tan, A.J. Butte, G.M. Weinstock, G. M. Slavich, E. Sodergren, T.L. McLaughlin, F. Haddad, M.P. Snyder, Nat. Med. 25 (2019) 792.

[3] M. Forhan, B.M. Zagorski, S. Marzonlini, P. Oh, D.A. Alter, Can. J. Diabetes 37 (2013) 189.

[4] T. Bruderer, T. Gaisl, M.T. Gaugg, N. Nowak, B. Streckenbach, S. Muller, A. Moeller, M. Kohler, R. Zenobi, Chem. Rev. 119 (2019) 10803.
[5] W. Miekisch, J.K. Schubert, G.F. Noeldge-Schomburg, Clin. Chim. Acta 347 (2004) 25.
[6] V. Ruzsányi, M. Péter Kalapos, J. Breath Res. 11 (2017), 024002.
[7] M.P. Kalapos, Biochim. Biophys. Acta 1621 (2003) 122.
[8] M. Statheropoulos, A. Agapiou, A. Georgiadou, J. Chromatogr. Biomed. Appl. 832 (2006) 274.
[9] V. Ruzsányi, M.P. Kalapos, C. Schmidl, D. Karall, S. Scholl-Bürgi, M. Baumann, J. Breath Res. 12 (2018), 036021.
[10] K. Musa-Veloso, S.S. Likhodii, S.C. Cunnane, Am. J. Clin. Nutr. 76 (2002) 65.
[11] J. King, A. Kupferthaler, K. Unterkofler, H. Koc, S. Teschl, G. Teschl, W. Miekisch, J. Schubert, H. Hinterhuber, A. Amann, J. Breath Res. 3 (2009), 027006.
[12] K. Königstein, S. Abegg, A.N. Schorn, I.C. Weber, N. Derron, A. Krebs, P.A. Gerber, A. Schmidt-Trucksäss, A.T. Güntner, J. Breath Res. 15 (2021), 016006.
[13] A.T. Güntner, N.A. Sievi, S.J. Theodore, T. Gulich, M. Kohler, S.E. Pratsinis, Anal. Chem. 89 (2017) 10578.
[14] B.T.E. Andrews, W. Denzer, G. Hancock, A.D. Lunn, R. Peverall, G.A.D. Ritchie, K. Williams, J. Breath Res. 12 (2018), 036015.
[15] A.T. Güntner, S. Abegg, K. Konigstein, P.A. Gerber, A. Schmidt-Trucksass, S. E. Pratsinis, ACS Sens. 4 (2019) 268.
[16] J.W. Yoon, J.H. Lee, Lab Chip 17 (2017) 3537.
[17] A.T. Güntner, M. Wied, N.J. Pineau, S.E. Pratsinis, Adv. Sci. 7 (2020), 1903390.
[18] S. Abegg, L. Magro, J. van den Broek, S.E. Pratsinis, A.T. Güntner, Nat. Food 1 (2020) 351.
[19] S.K. Kundu, J.A. Bruzek, R. Nair, A.M. Judilla, Clin. Chem. 39 (1993) 87.
[20] B.E. Landini, S.T. Bravard, IEEE Sens. J. 9 (2009) 1802.
[21] M.-Y. Chuang, Y.-T. Lin, T.-W. Tung, L.-Y. Chang, H.-W. Zan, H.-F. Meng, C.-J. Lu, Y.-T. Tao, Sens. Actuators B 260 (2018) 593.
[22] D. Wang, F. Zhang, A. Prabhakar, X. Qin, E.S. Forzani, N. Tao, ACS Sens. 6 (2021) 450.
[23] H.-J. Cho, S.-J. Choi, N.-H. Kim, I.-D. Kim, Sens. Actuators B 304 (2020), 127350.
[24] R. Yoo, A.T. Güntner, Y. Park, H.J. Rim, H.-S. Lee, W. Lee, Sens. Actuators B 283 (2019) 107.
[25] Y.-M. Jo, K. Lim, H.J. Choi, J.W. Yoon, S.Y. Kim, J.-H. Lee, Sens. Actuators B 325 (2020), 128821.
[26] L. Wang, A. Teleki, S.E. Pratsinis, P.I. Gouma, Chem. Mater. 20 (2008) 4794.
[27] M. Righettoni, A. Tricoli, S.E. Pratsinis, Chem. Mater. 22 (2010) 3152.
[28] H.J. Choi, J.-H. Chung, J.-W. Yoon, J.-H. Lee, Sens. Actuators B 338 (2021), 129823.
[29] I.C. Weber, H.P. Braun, F. Krumeich, A.T. Güntner, S.E. Pratsinis, Adv. Sci. 7 (2020), 2001503.
[30] I.C. Weber, A.T. Güntner, Sens. Actuators B 356 (2022), 131346.
[31] T. Toyooka, S. Hiyama, Y. Yamada, J. Breath Res. 7 (2013), 036005.
[32] A.T. Güntner, N.J. Pineau, P. Mochalski, H. Wiesenhofer, A. Agapiou, C. A. Mayhew, S.E. Pratsinis, Anal. Chem. 90 (2018) 4940.
[33] N.J. Pineau, J.F. Kompalla, A.T. Güntner, S.E. Pratsinis, Microchim. Acta 185 (2018) 563.
[34] A.T. Güntner, J.F. Kompalla, H. Landis, S.J. Theodore, B. Geidl, N.A. Sievi, M. Kohler, S.E. Pratsinis, P.A. Gerber, Sensors 18 (2018) 3655.
[35] I.C. Weber, N. Derron, K. Königstein, P.A. Gerber, A.T. Güntner, S.E. Pratsinis, Small Science 1 (2021), 2100004.
[36] M. Righettoni, A. Tricoli, S. Gass, A. Schmid, A. Amann, S.E. Pratsinis, Anal. Chim. Acta 738 (2012) 69.
[37] I.C. Weber, C.-t Wang, A.T. Güntner, Materials 14 (2021) 1839.
[38] A.T. Güntner, N.J. Pineau, S.E. Pratsinis, Prog. Energy Combust. Sci. 90 (2022), 100992.
[39] A.M. Ellis, C.A. Mayhew, Proton Transfer Reaction Mass Spectrometry: Principles and Applications, John Wiley & Sons, 2013.
[40] D.P. Swain, K.S. Abernathy, C.S. Smith, S.J. Lee, S.A. Bunn, Med. Sci. Sports Exerc. 26 (1994) 112.
[41] V.F. Froelicher, J.N. Myers, Exercise and the Heart, W.B. Saunders Company, Philadelphia, 2000.
[42] World Health Organization, Geneva: World health organization, 1999.
[43] S. Schon, S.J. Theodore, A.T. Güntner, Sens. Actuators B 273 (2018) 1780.
[44] S. American Thoracic, S. European Respiratory, Am. J. Respir. Crit. Care Med. 171 (2005) 912.
[45] F. Di Francesco, C. Loccioni, M. Fioravanti, A. Russo, G. Pioggia, M. Ferro, I. Roehrer, S. Tabucchi, M. Onor, J. Breath Res. 2 (2008), 037009.
[46] IONICON PTR-ToF-MS 1000, *Technical Datasheet*, ⟨https://www.ionicon.com/series/details/ptr-ms-trace-voc-analyzers?gclid=EAIaIQobChMIuZ7CwviS9wIVBp53Ch2Xkg-oEAAYASAAEgI_YPD_BwE⟩ (Accessed: 25 April 2022).
[47] J. Herbig, M. Muller, S. Schallhart, T. Titzmann, M. Graus, A. Hansel, J. Breath Res. 3 (2009), 027004.
[48] A. Jordan, S. Haidacher, G. Hanel, E. Hartungen, L. Märk, H. Seehauser, R. Schottkowsky, P. Sulzer, T. Märk, Int. J. Mass Spectrom. 286 (2009) 122.
[49] A.T. Güntner, M. Righettoni, S.E. Pratsinis, Sens. Actuators B 223 (2016) 266.
[50] M. Müller, T. Mikoviny, S. Feil, S. Haidacher, G. Hanel, E. Hartungen, A. Jordan, L. Märk, P. Mutschlechner, R. Schottkowsky, P. Sulzer, J.H. Crawford, A. Wisthaler, Atmos. Meas. Tech. 7 (2014) 3763.
[51] J.M. Bland, D.G. Altman, Lancet 327 (1986) 307.
[52] I.B. Hirsch, Med. Clin. N. Am. 82 (1998) 689.
[53] K. Schwarz, A. Pizzini, B. Arendacka, K. Zerlauth, W. Filipiak, A. Schmid, A. Dzien, S. Neuner, M. Lechleitner, S. Scholl-Burgi, W. Miekisch, J. Schubert, K. Unterkofler, V. Witkovsky, G. Gastl, A. Amann, J. Breath Res. 3 (2009), 027003.
[54] J.W. Gardner, Semicond. Sci. Technol. 4 (1989) 345.
[55] J.W. Gardner, Sens. Actuators B 1 (1990) 166.
[56] A. Dahshan, K. Donovan, J. Pediatr. Gastroenterol. Nutr. 33 (2001) 214.
[57] J. van den Broek, P. Mochalski, K. Königstein, W.C. Ting, K. Unterkofler, A. Schmidt-Trucksäss, C.A. Mayhew, A.T. Güntner, S.E. Pratsinis, Sens. Actuators B 357 (2022), 131444.
[58] P. Trefz, J. Obermeier, R. Lehbrink, J.K. Schubert, W. Miekisch, D.-C. Fischer, Sci. Rep. 9 (2019) 15707.
[59] G.F. Cahill Jr., Annu. Rev. Nutr. 26 (2006) 1.
[60] J.C. Anderson, Obesity 23 (2015) 2327.
[61] L.R. Saslow, S. Kim, J.J. Daubenmier, J.T. Moskowitz, S.D. Phinney, V. Goldman, E. J. Murphy, R.M. Cox, P. Moran, F.M. Hecht, PLoS One 9 (2014), e91027.
[62] M.J. Sulway, J.M. Malins, Lancet 2 (1970) 736.
[63] C. Kramer, P. Mochalski, K. Unterkofler, A. Agapiou, V. Ruzsanyi, K.R. Liedl, J. Breath Res. 10 (2016), 017103.
[64] P. Puchalska, P.A. Crawford, Cell Metab. 25 (2017) 262.
[65] American Diabetes Association, Diabetes Care 42 (2019) S13.

Andreas T. Güntner has a M.Sc. (2014), a Ph.D. (2016) in Mechanical Engineering from ETH Zürich. Currently, he is a team leader at the University of Zürich/University Hospital Zürich and will launch the Human-centered Sensing Laboratory as assistant professor at ETH Zürich in the Fall of 2022. His research advances the fundamental understanding on micro & nanosystems and their utilization for sensing applications in healthcare, environmental and food-related fields. Andreas' research has been recognized by an ERC Starting Grant 2021, two ETH Medals and the Excellence Award for Product Design and Engineering from the European Federation of Chemical Engineering among other recognitions.

Ines C. Weber received her B.Sc. (2016) and M.Sc. (2018) in material science and her Ph. D. in mechanical engineering (2022) from the Swiss Federal Institute of Technology (ETH Zurich). Her research centers around highly selective gas sensors enabled through filters for healthcare and environmental applications. For this, she received the BRIDGE Proof of Concept grant as well as a student presentation prize at the International Meeting on Chemical Sensors 2021 and a poster award at the European Aerosol Conference 2021. Today, she focuses on the integration of sensors into handheld devices and tests in medical and lifestyle applications, in close collaboration with the University Hospital Zurich.

Sotiris E. Pratsinis https://ptl.ethz.ch/ (diploma in chemical engineering from Aristotle University of Thessaloniki, Greece (1977) and Ph.D. from University of California, Los Angeles (1985)). He was in the faculty of the University of Cincinnati (1985–2000) till elected professor of Process Engineering & Materials Science at ETH Zurich (1998-now). He focuses on the fundamentals of aerosols and the assembly of gas sensors for environmental and life science applications. He has graduated 45 Ph.Ds, published 400+ refereed articles, filed 20+ patents licensed to industry that have contributed to creation of four spinoffs. One of them entered the LSE in late 2020.

Philipp A. Gerber (M.D. (2005) and M.Sc. degree in Medical Biology (2007) at the University of Zurich) completed his postgraduate training in internal medicine and endocrinology at the University Hospital Zurich. He conducted two post-doctoral research stays in basic metabolic research at ETH Zurich as well as at Imperial College London. He returned to the University Hospital Zurich, where he is currently working as a senior physician and group leader at the Department of Endocrinology. His research focuses on clinical studies in nutrition, with a particular interest in the impact of the composition and timing of nutrition on metabolic diseases.